

Isolated Rotor Engagement and Disengagement Simulations in Ship Airwake

M. Groom¹, B. Thornber¹, G.A. Vio¹ and R. Widjaja²

¹School of Aerospace, Mechanical and Mechatronic Engineering
University of Sydney, New South Wales 2006, Australia

²Defence Science and Technology Group
Fishermans Bend, Victoria 3207, Australia

Abstract

During the engagement and disengagement phases of maritime helicopter operations, a transient aeroelastic phenomenon can occur, known as blade sailing. Characterised by large blade deflections, which have the potential to cause structural damage to the aircraft, blade sailing can limit the tactical flexibility of a helicopter operating in a maritime environment by restricting the wind and sea conditions in which engagement and disengagement can occur. The ship airwake has been identified as being a major factor in the blade sailing phenomenon, however previous research has either been limited to a small range of wind conditions or has used simple deterministic solutions of too low fidelity to be considered truly representative of the actual airwake.

In this paper, numerical simulations are conducted to understand how the ship airwake can affect transient rotor response, so as to assist in defining engagement and disengagement operating limits. An analysis is developed using FLIGHTLAB, and the ship airwake is represented by RANS solutions computed using OpenFOAM for a generic ship geometry. The results are interesting and significant to the operation of a shipboard helicopter. Based on the current research, comments on the implications of results for ship-helicopter operations are welcome.

Introduction

The act of operating a helicopter on or near the flight deck of a moving ship, that could be experiencing quite high sea states, carries an inherent risk. The nature of the ship airwake also means that the helicopter may be operating in quite a challenging aerodynamic environment, particularly for high wind conditions. With the addition of other factors such as low visibility and sea-spray, this makes the pilot workload in these situations greater than during equivalent land-based operations. The study of these situations, known as the Ship-Helicopter Dynamic Interface, aims to predict the behaviour of the helicopter for a given set of conditions and thereby reduce any risks associated with them.

Challenges and risks associated with shipboard helicopter operations are not restricted to just take-off and landing, with the potential for problems to occur even before the helicopter takes off from or after it lands on the flight deck. In particular, during the engagement and disengagement of the rotor, excessive flapwise deflections of the rotor blades can occur. This is an aeroelastic phenomenon known as blade sailing [1], that can have considerable consequences for both the structural integrity of the rotorcraft and the health and safety of surrounding operators [2].

The blade sailing phenomenon was first studied in the 1960's [3], however the theoretical component of this work was limited to purely analytical methods, due to a lack of computing power at the time. The complex nature of the blade sailing phenomenon necessitates the use of numerical methods to simulate

the transient rotor behaviour, with blade sailing research at the University of Southampton the first to adopt this approach [4]. The initial theoretical model that was developed was extended to include both hingeless and articulated rotor types [5, 6], with wind-tunnel tests of a radio-controlled model helicopter also used to verify the results [7]. This research was the first of its kind to include the effects of a realistic ship airwake on the transient rotor response, however the variation in ship airwake with wind-over-deck (WOD) angle, and the subsequent effect this has on blade sailing behaviour, was not explored.

Further research on blade sailing was conducted at Pennsylvania State University [8], where a more detailed, finite element based model of the transient rotor response during shipboard engagement and disengagement operations was developed. Drop tests of an articulated model rotor blade were performed to validate the theoretical predictions of transient blade response during a droop stop impact [9], with the theoretical model also extended to investigate the feedback control of gimballed tiltrotors undergoing shipboard engagement [10].

Most recently, advanced modelling techniques for studying blade sailing were developed at Carleton University [11]. This research focused on discrete rigid-body modelling with experimentally correlated turbulence [12, 13], and using a geometrically-exact, intrinsic formulation for thin-walled beams to investigate the use of integral active twist as a means of controlling the blade sailing phenomenon [14, 15, 16]. The influence of representative ship motion on the aeroelastic rotor response was also investigated [17], both experimentally and with numerical simulation.

Previous attempts to accurately represent the effects of the ship airwake in engagement and disengagement simulations have all been limited in some form. The use of simple deterministic distributions (such as those used in [8]) allow for a wide range of wind conditions to be simulated, however they are too simplistic in nature to be considered a realistic representation. On the other hand, the use of experimentally measured airwake data (such as that used in [11]) can give a very accurate representation, but only for the specific case that it was measured for.

The use of CFD solutions of the ship airwake is a useful alternative in this regard, which was the approach used in the research in [18]. This approach forms the basis for this current research, which uses CFD solutions of the ship airwake to investigate a wide range of wind conditions, and the impact they have on the transient aeroelastic response of an isolated rotor undergoing engagement and disengagement. This is necessary for the determination of the Ship-Helicopter Operational Limits (SHOLs) for this particular type of dynamic interface operation.

Modelling Approach

As mentioned above, the modelling approach used in this research was based on that used in [18]. An aeroelastic model of a generic isolated articulated rotor was developed and simulated using the rotorcraft simulation software FLIGHTLAB. The ship airwake data used in these simulations was provided from CFD solutions of the airwake around a generic ship geometry, known as the Simplified Frigate Shape (SFS), that were computed using OpenFOAM. Each aspect of the modelling process is described in detail in the sections below.

Isolated Rotor

The rotor that was chosen to be modelled was a generic fully articulated rotor, with properties based on those from a baseline rotor model used in engagement/disengagement research at the Pennsylvania State University [19], itself a simplified version of a CH-46 rotor. A table of the relevant properties of this rotor is given in Table 1.

| Property | Value |
|---------------------------|----------------|
| No. of blades | 4 |
| Full rotor speed | 30 rad/s |
| Blade length | 7.62 m |
| Blade chord | 0.4572 m |
| Effective blade twist | -10° |
| Root cutout | 1.524 m |
| Flap hinge offset | 0.1905 m |
| Lag hinge offset | 0.381 m |
| Feathering hinge offset | 0.5715 m |
| Flap/droop stop locations | $\pm 1^\circ$ |
| Lead/lag stop locations | $\pm 10^\circ$ |

Table 1: Properties of the generic isolated rotor.

Using the radial distributions of inertial and stiffness properties (given in [19]), the blades of the isolated rotor were modelled in FLIGHTLAB with nonlinear beam finite elements, whose formulation is based on that given in [20]. A verification study was performed to determine the suitable number of finite elements, which was found to be 20 per blade. As per the research in [19], a modal reduction was employed to reduce computational cost, with 12 modes found to be appropriate. A damping ratio was also applied to each mode, calculated by assuming the damping to be proportional.

The airloads on each blade were calculated with a quasi-steady empirical aerodynamic model for a NACA 0012 section, based on curve-fits of experimental data from [21, 22]. The model includes stall and post-stall effects, as well as Mach number effects on the lift and drag coefficients. The dynamic inflow model of Peters & He [23] was used to calculate the induced velocity through the rotor disk, with 6 modal inflow states used.

The flap/droop stops (as well as the lead/lag stops) were modelled with a nonlinear rotational spring and damper at each hinge, implemented in FLIGHTLAB with a table lookup. A plot of the nonlinear stiffness curve for the flap hinge rotational spring is shown in Figure 1.

Ship Airwake

The SFS geometry, shown in Figure 2, was originally conceived as part of The Technical Cooperation Program AER-TP2 and has previously been used to produce a representative ship airwake in the blade sailing research in [19]. The CFD solutions of the airwake of the SFS were computed on a structured mesh consisting of 4 million cells that had already been developed in concurrent research at the University of Sydney, with de-

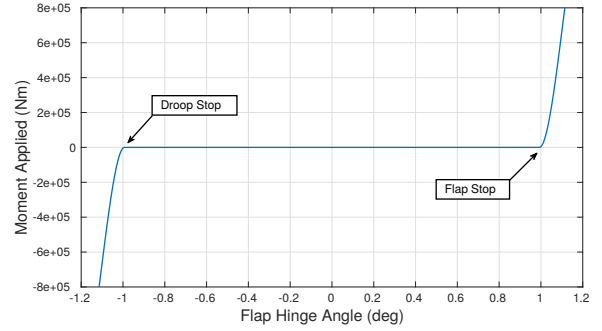


Figure 1: Stiffness curve for the flap hinge rotational spring.

tails of the validation of the mesh found in [24]. For WOD speeds of 30, 40 and 50 knots and WOD directions in 30° increments, the steady-state solution of the incompressible RANS equations with a Spalart-Allmaras turbulence model was computed in OpenFOAM.

Some additional time-accurate simulations were also run for the 0° and 180° cases, as the bluff-body vortex shedding exhibited at these WOD angles often resulted in unsatisfactory steady-state convergence. The results of these simulations were time-averaged and used in the same manner as the other steady airwake solutions once imported into FLIGHTLAB.

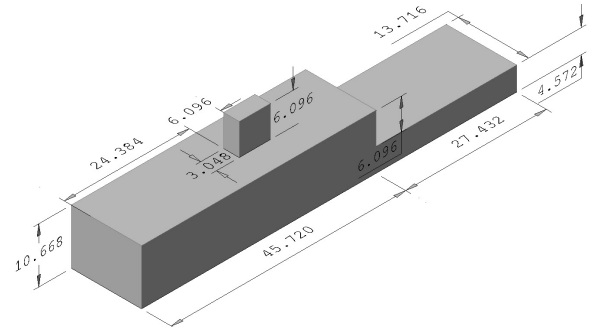


Figure 2: The Simplified Frigate Shape Geometry. All dimensions are in meters.

To illustrate the level of fidelity of the CFD solutions some flow visualisation, in the form of isosurfaces of the Q-criterion for vortex identification, is shown in Figure 3 for the 50 knot, 0° WOD case. This particular plot is a good illustration of the bluff-body vortex shedding in the airwake that is typical for this WOD angle.

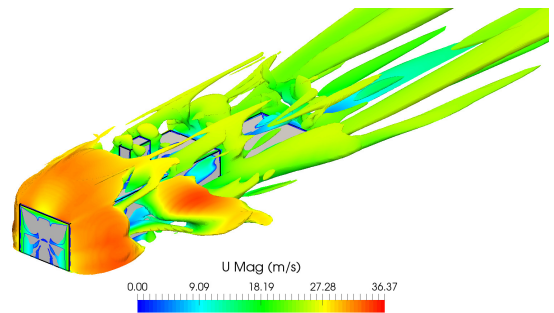


Figure 3: Isosurfaces of Q-criterion over the SFS at 50 knots, 0° WOD angle, coloured by velocity magnitude.

Engagement and Disengagement Simulations

Using the airwake data extracted from the CFD solutions for the SFS, simulations of the engagement and disengagement of the isolated rotor were performed in FLIGHTLAB for a specified rotor speed profile. Both the engagement and disengagement rotor speed profiles were given by simple sinusoids over a 20 second interval. The rotor speed profiles for both the engagement and disengagement simulations are given in Equation 1.

$$\Omega(t) = \frac{\Omega_{max}}{2} \left(\cos\left(\pi \frac{t}{20} + \pi\right) + 1 \right) \quad \text{engagement} \quad (1)$$

$$\Omega(t) = \frac{\Omega_{max}}{2} \left(\cos\left(\pi \frac{t}{20}\right) + 1 \right) \quad \text{disengagement}$$

For the engagement simulations, in addition to the 20 second interval of increasing rotor speed, an extra period of time was included at the start of the simulation where the rotor was at rest. This was to allow the rotor blades to settle on the droop stops, which in turn meant that the blades would have the correct initial deflection once the engagement started. The control settings of the rotor used for all of the simulations are shown in Table 2. These were held constant throughout the engagement and disengagement process. The initial azimuthal angle of the rotor is also given.

| Property | Value |
|---------------------------|-------|
| Collective pitch | 4° |
| Lateral cyclic pitch | 0° |
| Longitudinal cyclic pitch | 4° |
| Blade 1 initial azimuth | 0° |

Table 2: Control settings for the engagement and disengagement simulations.

In order to determine the effect the addition of the ship airwake has on the transient rotor response, an initial round of simulations was performed in a uniform horizontal wind, with the flapwise tip deflections of the rotor blades during both engagement and disengagement recorded. Figures 4 and 5 show the time history of these flapwise tip deflections, non-dimensionalised with respect to the blade length R , for a 50 knot, 300° wind.

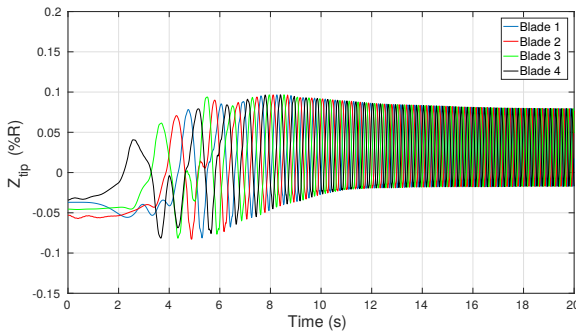


Figure 4: Flapwise tip deflections during engagement in a horizontal 50 knot, 300° wind.

Of the most concern from an operational standpoint are the maximum upward and downward flapwise tip deflections, in particular the downward tip deflections as these can result in blade-fuselage impacts in severe cases. For the engagement and disengagement shown in Figures 4 and 5, the maximum downward tip deflections are 8.28% R and 9.80% R , which occur at 14.0% and 7.91% of the full rotor speed respectively.

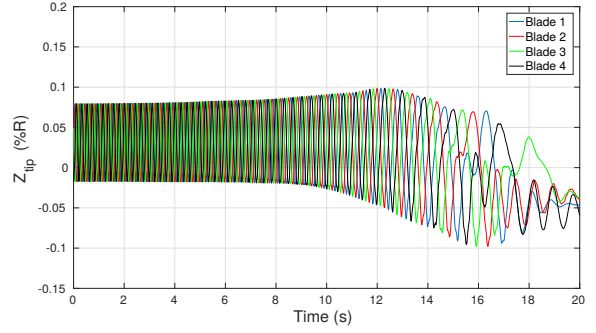


Figure 5: Flapwise tip deflections during disengagement in a horizontal 50 knot, 300° wind.

For the simulations with the ship airwake included, three landing spots on the SFS flight deck were analysed. These were at 9.144 m, 18.288 m and 27.432 m aft of the hangar, along the ship centreline and at a height of 4.877 m above the flight deck. Figures 6 and 7 show the time history of flapwise tip deflections during engagement and disengagement at the first of these landing spots, for the same base wind conditions as Figures 4 and 5.

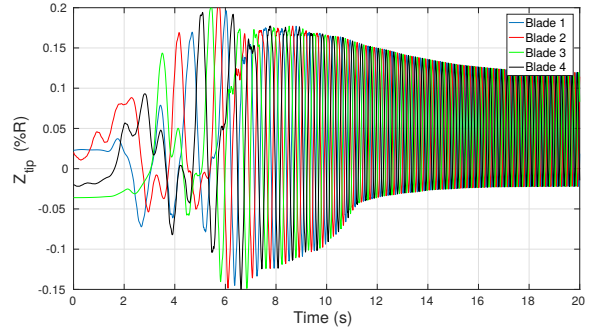


Figure 6: Flapwise tip deflections during engagement at SFS landing spot 1 in a 50 knot, 300° wind.

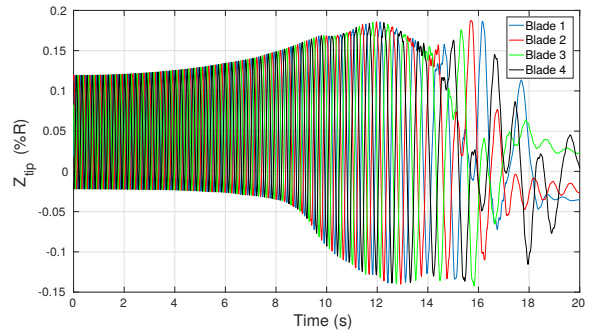


Figure 7: Flapwise tip deflections during disengagement at SFS landing spot 1 in a 50 knot, 300° wind.

When comparing the response in Figures 6 and 7 with that in Figures 4 and 5, the exacerbating effect of the ship airwake environment on the flapwise blade motions is obvious. The maximum downward tip deflections are now 15.0% R and 14.2% R , and these occur at 24.7% and 10.4% of the full rotor speed. This is due mainly to the additional out-of-plane velocities present in the airwake at the rotor disk. These generate larger aerodynamic forces on the blades while the centrifugal stiffening effect remains the same, resulting in larger out-of-plane blade motions.

Conclusions

The results of the engagement and disengagement simulations at the three landing spots aboard the SFS, of which one case is presented here, demonstrated the impact the ship airwake environment can have on the transient response of the rotor. In particular, the largest flapwise tip deflections occurred in regions of the flow field that had large out-of-plane velocities, which was in agreement with the findings of previous research. This highlights the need for accurate modelling of the airwake over the entire range of operational conditions, either via experimental or computational techniques.

While a large number of different cases were analysed in this research, there are still a number of limitations that should be addressed in future work. The fidelity of these simulations could be increased with the inclusion of the effects of ship dynamics, such as has been the focus of previous studies, as well as a more detailed investigation into different control settings and a more realistic representation of the rotor speed profile. Improvements could also be made to the representation of the ship airwake, through the inclusion of an unsteady flow field or the effects of an atmospheric boundary layer.

Acknowledgements

The authors wish to acknowledge the Defence Science and Technology Group for providing funding and assistance for this research.

References

- [1] Newman, S., The Phenomenon of Helicopter Rotor Blade Sailing, *Journal of Aerospace Engineering*, **213**, 1999, 347–363.
- [2] Newman, S., The Safety of Shipborne Helicopter Operation, *Aircraft Engineering and Aerospace Technology*, **76**, 2004, 487–501.
- [3] Leone, P.F., Theoretical and Experimental Study of the Flap Droop Stop Impact Transient Aeroelastic Response of a Helicopter Rotor Blade, *Journal of the American Helicopter Society*, **9**, 1964, 32–37.
- [4] Hurst, D.W. and Newman, S.J., Wind-Tunnel Measurements of Ship Induced Turbulence and the Prediction of Helicopter Rotor Blade Response, *Vertica*, **12**, 1988, 267–278.
- [5] Newman, S.J., A Theoretical Model for Predicting the Blade Sailing Behaviour of a Semirigid Rotor Helicopter, *Vertica*, **14**, 1990, 531–544.
- [6] Newman, S.J., The Application of a Theoretical Blade Sailing Model to Predict the Behaviour of Articulated Helicopter Rotors, *Aeronautical Journal*, **96**, 1992, 233–239.
- [7] Newman, S.J., The Verification of a Theoretical Helicopter Rotor Blade Sailing Method by Means of Wind-tunnel Testing, *Aeronautical Journal*, **99**, 1995, 41–51.
- [8] Geyer, W.P., Smith, E.C. and Keller, J.A., Aeroelastic Analysis of Transient Blade Dynamics During Shipboard Engage/Disengage Operations, *Journal of Aircraft*, **35**, 1998, 445–453.
- [9] Keller, J.A. and Smith, E.C., Experimental and Theoretical Correlation of Helicopter Rotor Blade-Droop Stop Impacts, *Journal of Aircraft*, **36**, 1999, 443–450.
- [10] Keller, J.A. and Smith, E.C., Active Control of Gimballing Rotors Using Swashplate Actuation During Shipboard Engagement Operations, *Journal of Aircraft*, **40**, 2003, 726–733.
- [11] Khouli, F., Afagh, F.F. and Langlois, R.G., Design, Simulation and Experimental Results for Flexible Rotors in a Ship Airwake, *Journal of Aircraft*, **53**, 2016, 262–275.
- [12] Wall, A.S., Langlois, R.G. and Afagh, F.F., Modeling Helicopter Blade Sailing: Dynamic Formulation in the Planar Case, *Journal of Applied Mechanics*, **74**, 2007, 1104–1113.
- [13] Wall, A.S., Afagh, F.F., Langlois, R.G. and Zan, S.J., Modeling Helicopter Blade Sailing: Dynamic Formulation and Validation, *Journal of Applied Mechanics*, **75**, 2008, 0610041–06100410.
- [14] Khouli, F., Langlois, R.G. and Afagh, F.F., Analysis of Active Closed Cross-Section Slender Beams Based on Asymptotically Correct Thin-Wall Beam Theory, *Smart Materials & Structures*, **16**, 2007, 221–229.
- [15] Khouli, F., Afagh, F.F. and Langlois, R.G., Application of the First Order Generalized-alpha Method to the Solution of an Intrinsic Geometrically Exact Model of Rotor Blade Systems, *Journal of Computational and Nonlinear Dynamics*, **4**, 2009, 1–12.
- [16] Khouli, F., Griffiths, J., Afagh, F.F. and Langlois, R.G., Actuation of Slender Thin-Wall Anisotropic Open Cross-Section Beams Based on Asymptotically Correct Vlasov Theory, *Journal of Intelligent Material Systems and Structures*, **21**, 2010, 529–540.
- [17] Khouli, F., Wall, A.S., Afagh, F.F. and Langlois, R.G., Influence of Ship Motion on the Aeroelastic Response of a Froude-Scaled Maritime Rotor System, *Ocean Engineering*, **54**, 2012, 170–181.
- [18] Kang, H., He, C. and Carico, D., Modeling and Simulation of Rotor Engagement and Disengagement During Shipboard Operations, In *60th Annual Forum Proceedings of the American Helicopter Society*, American Helicopter Society, 2004, 315–324.
- [19] Keller, J.A., Analysis and Control of the Transient Aeroelastic Response of Rotors During Shipboard Engagement and Disengagement Operations, Ph.D. Thesis, The Pennsylvania State University, Department of Aerospace Engineering, 2001.
- [20] Danielson, D. and Hodges, D., A Beam Theory for Large Global Rotation, Moderate Local Rotation, and Small Strain, *Journal of Applied Mechanics*, **55**, 1988, 179–184.
- [21] Prouty, R.W., *Helicopter Performance, Stability, and Control*, Robert E. Krieger Publishing Co., 1990.
- [22] Critzos, C.C., Heyson, H.H. and Boswinkle, R.W., Aerodynamic Characteristics of NACA 0012 Airfoil Section at Angles of Attack from 0° to 180°, NACA TN-3361, National Advisory Committee for Aeronautics, 1955.
- [23] Peters, D.A. and He, C.J., Correlation of Measured Induced Velocities with a Finite-State Wake Model, *Journal of the American Helicopter Society*, **36**, 1991, 59–70.
- [24] Linton, D., Thornber, B. and Widjaja, R., A Study of LES Methods for Simulation of Ship Airwakes, In *46th AIAA Fluid Dynamics Conference*, AIAA Aviation, 2016.